

# LIGHT CURVE MODEL VALIDATION BY CROSS-COMPARISON WITH PHOTOMETRIC DATA FOR SPACE OBJECT CHARACTERISATION

A. Petit, H. Tarrieu, L. Duthil, A. Rolin, and D. Giolito

Share My Space, 14 rue Crespin du Gast, 75011 Paris, France

Email: alexis.petit, henri.tarrieu, lea.duthil, alexis.rolin, damien.giolito@sharemyspace.space

## ABSTRACT

With the emergence of the new space industry came a sky-rocketing rise of the Earth-orbiting object population, creating unprecedented challenges for space operations. More than 1 million debris greater than 1 cm pose a threat to current and future space-based activities. They have to be tracked and characterized in order to minimize collision risks and help find solutions towards a sustained outer space.

On top of providing astrometric data, optical observations of Resident Space Objects (RSO) uniquely offer the ability to retrieve the photometric behavior of such objects. Images produced by Share My Space's ground-based telescope network allow the extraction of the luminous flux of an object over a certain time span: assuming the choice of an appropriate sampling rate, we call such measurements light curves. This information finds applications on several subjects: notably for RSO attitude determination, as well as the validation of the photometric chain model relative to Share My Space's observatories.

We present two methods for light curves extraction through both passive and active observations. In sidereal tracking, the passive method consists in waiting for the object to travel through the field of view of the instrument to capture its passage. The RSO forms a light streak moving through a series of consecutive images, from which we measure the flux along the trajectory. With active object tracking, images are acquired at higher framerates, forming a point-like object on captures of RSO, showing streak-like stars in the background.

We compare these two ways of extracting light curves, expecting an agreement between variables (flux, characteristic periods) measured using both methods. This also helps raise particular observing scenarios that would favor one of the two methods: with small or distant objects for example. These results are confronted to predictions made by our photometric model, allowing the verification of the simulation algorithms used, as well as their refinement through the addition of new attitude parameters. Performing light curve analysis of some well-known objects, such as SLR satellites, provides references for the validation of the photonic chain model.

After building confidence in our measurements, we can explore the practical applications to our light curves. Mainly, this data can help assess the attitude of observed objects: when compared to a set of known behaviors computed by the photonic chain model, light curves can characterize a spinning object by fitting the closest theoretical match to it. By Fourier Transform analysis, and including Bidirectional Reflectance Distribution Function (BRDF) modelling, parameters like the main rotational period and the orientation of each rotation axis can be determined. This information, combined with astrometric positional RSO data, helps us better anticipate an object's behavior through time, allowing safer and easier satellite operations.

With the growth of Share My Space's observation station network, we aim at enriching our catalog with light curves for each object tracked, pushing optical detection methods to their full potential.

Keywords: telescope; satellites & space debris; light curve.

## 1. INTRODUCTION

Since the seventeenth century, telescopes are a privileged way to observe and measure positions of celestial bodies. During the twentieth century, other methods have been invented like radars or laser. For the case of artificial space objects, all approaches are very complementary, each having their pros and cons.

However, during these past few years, technologies have evolved, leading to a new generation of optical setups taking advantage of telescopes combining large aperture and large field of view, associated to large CMOS sensors. Such devices are available off the shelf at reasonable prices. Subsequently, a new strong interest for optical systems relative to space object tracking from LEO to GEO regions, and beyond, [1] has emerged. For these reasons it is worth investigating the capacity to observe the smallest objects.

Share My Space operates a network of observatories with

telescopes. Installed in November 2020, the setup at Baronnies provençales (in Figure 1) is based on a RASA 14 telescope (aperture of 36 cm). Daily observations are conducted to track space objects from LEO to GEO regions. It was shown that objects as small as cubesats at 500 km of altitude can be detected. In Figure 2, the streak created by the 0.25U cubesat SPACEBEE (#44370), with a size of  $10 \times 10 \times 2.5$  cm, crossing the telescope field of view is plotted.



Figure 1. Observatory located at Baronnies provençales and operated by Share My Space.

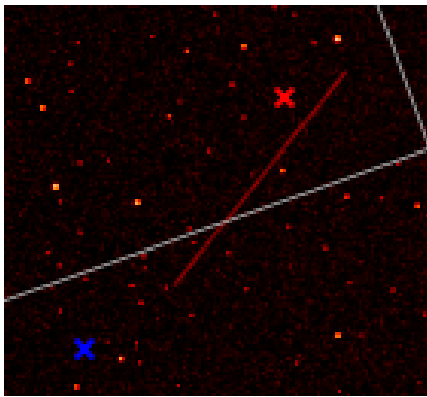


Figure 2. cubesat SPACEBEE observed with a telescope RASA 14. The red and blue crosses are the begin and end of streak predicted using the last TLE.

In previous works, the performance of space objects detection has been challenged with a complete model of the photon chain, from the light emitted by the Sun and reflected by the satellite to the camera [2]. This ongoing work is done using new observation data (such as light curves) and calibration campaigns, for example, to char-

acterize the sky. The main motivation is our capacity to extrapolate this detection performance of larger telescopes.

In this paper, we study the photon chain, which allows to assess the performance of larger telescopes. In Section 2, we introduce our model of the photon chain. In Section 3, we use photometric data to validate the model based on measures of the sky background, streaks of space objects, and light curves. In Section 4, we extrapolate the performance of a telescope of 1 m of aperture. In Section 5, we investigate the attitude model. Finally, in Section 6 we draw some conclusions about future observation campaigns with telescopes.

## 2. MODEL OF THE PHOTON CHAIN

An object is detected on the condition that the signal-to-noise ratio (SNR) is above a limit threshold. Hence, we need to compute the measured signal due to the space object and the measured signal due to the sky background and the noise of the camera. In this Section, each stage of the photon model is introduced in order to compute all contributions to the signal measured by the image.

### 2.1. General overview

The model is based on the computation of the light quantity received by the sensor and converted into a measurable unit which is the number of Analog-Digital Units (ADUs) in the .fits image. The contributions of the sky background and the satellite are computed following three main stages described below:

- First, the quantity of light reflected by the satellite depends on the reflection law, the properties of the satellite surface and the geometry of the Sun, the satellite and the observer.
- Second, the light collected depends on the aperture of the telescope, the exposure time. But part of the light is also lost by the atmospheric absorption, the transmittance ratio of optics, and the quantum efficiency which all depend on the wavelength.
- Third, the signal in electrons is read by the camera and converted to ADUs taking into account setting parameters like the offset and the gain. At this stage the dark current and the readout noise are included.

### 2.2. Sky background

The luminosity of the sky is the main limitation for optical observations. The site of observation has to be chosen to offer the best conditions. However, the presence of the Moon cannot be avoided and has to be considered. The

model of sky magnitude provided by [3] takes into account the phase of the Moon, the angular distance from the Moon, the altitude angle of the considered position in sky, the Moon elevation angle and the magnitude of the sky at the zenith for a moonless night. In Figure 3, the magnitude of the sky computed with the model is plotted as a function of the azimuth and the altitude. Around the Moon located at 26 degrees of altitude and with a phase of 32 degrees (waxing crescent), the magnitude strongly decreases.

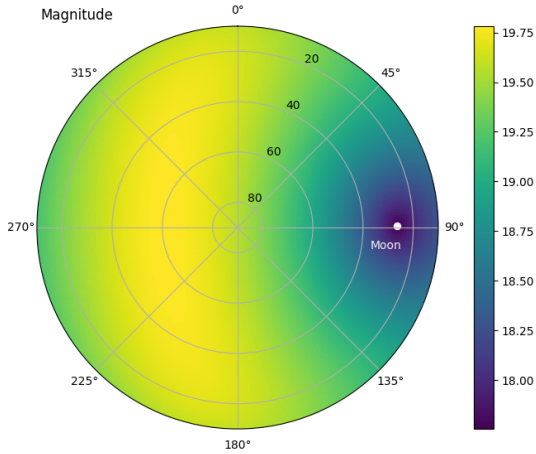


Figure 3. Modeled sky magnitude at the site of Baronniez provençales. The Moon is located at 26 degrees of altitude and 89 degrees of azimuth for the date of 2023/01/09 at 21:21:21.

### 2.3. Light reflected by a space object

Predicting the photonic flux of a satellite is also required to assess its detectability. To do so, it is necessary to simulate the space object passage in the sky to extract its local elevation, as increasingly more light reflected by the object will be absorbed by the atmosphere when decreasing in elevation.

Its geocentric position is also required to compute its phase angle, that can be described as the solid angle between the incident solar rays hitting the space object and the ones reflected by its surface in the direction of the observer. More robust models such as the Bi-Reflective Diffuse Function used for light curves simulation demand further parameters to take into account, such as the normal surface vector of each face of the space object.

The last parameter needed, considering the reflected light spectrum to be the same as the Sun, is the albedo of the space object to characterize its reflectance/absorption in the visible spectrum.

### 2.4. Camera characterisation

Theorizing the response of the camera is one of the most crucial steps to simulating the detection of satellites, as it is the final step prior to obtaining the image that will

thereafter be processed. It is important to differentiate both the intrinsic properties and the settings of the camera, as the settings can vary to render a completely different image.

The most critical intrinsic property of the camera is its quantum efficiency, which can be considered as the conversion rate from photons to electrons for each wavelength the sensor is set to detect. Other parameters include pixel length and the number of pixels per row/column.

Setting the camera requires deep knowledge of the settings, what they represent, and how to optimize them.

The most important of all is the Gain setting, as it sets the conversion rate from electron to ADU (or counts). ADU values give the shades of grey for each pixel on the image. However, this conversion rate is not always linear and varies according to the number of electrons present in each photosite and the Gain Setting used. It thus necessitates to be characterized for each Gain Setting wanted for observations, and for each camera. The Gain Setting also sets the readout noise.

Data is important. As it is desired to lose as little as possible, an Offset Setting is often applied to the camera, so that the irregularities in the photosites' detection threshold are blended. This is done by precharging the photosites prior to the capture, so that all pixels are charged above their threshold value.

An additional parameter can be used to increase the signal, by using Binning, i.e grouping pixels together so that the satellite will spend more time on each bin, thus increasing the integration time of the photons. This setting is most relevant when performing passive observations.

## 3. COMPARISONS OF THE MODEL WITH PHOTOMETRIC DATA

Observation campaigns have been conducted for two years. Two modes are used: passive observation where the satellite appears like a streak, and tracking observation where the satellite appears like a dot. The tracking mode allows to obtain luminosity measurement series of a few minutes or more.

### 3.1. Sky quality

The magnitude of the sky can be measured by an extraction of the mean flux of the background in images, and computed after the astrometric and photometric reduction. We propose to compare the measured magnitude with the predicted magnitude of our background model. For this purpose, we sample images of the sky distributed in azimuth and elevation. For each image, a value of the sky magnitude is computed and compared with our model. The difference is plotted in Figure 4.

The measured magnitude differs from the model due to the atmospheric transmittance which is affected by al-

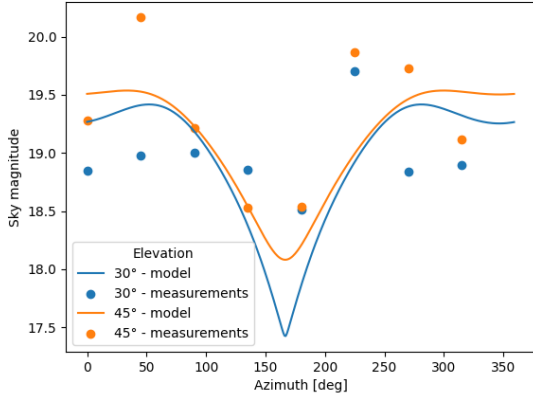


Figure 4. Difference between predicted and measured background magnitude. The atmospheric extinction coefficient has been set to  $k = 0.5$ .

titude, humidity, dust, aerosol, and precipitable water vapour (PWV).

### 3.2. Historical streak measurements

During each observation night, astrometric and photometric data of observed objects are recorded. It includes celestial angular coordinates (right ascension and declination in the topocentric frame), streak magnitude, the values in ADU of the background and the streak. Moreover, metadata like the gain and the offset camera settings are saved. Each observation of catalogued objects made in the past enables us to compute theoretical flux of the background and the streak, and compare it with the measurements.

In Figure 5, the flux measured for the observed streak of the satellite JASON 3(#41240) are compared to the flux computed by the model. We find a good agreement except for a few measures whose the theoretical flux is overestimated, mostly due to the attitude that is not taken into account.

### 3.3. Light curves

The variation of brightness can be measured over a short period by extracting the flux along a streak. The advantage is the accuracy of the temporal sampling which depends on the transit time in the individual field of view of a pixel. However, the duration of the light curve is limited to the exposure time. The other alternative is to track the object in the sky during its transit, and to acquire series of images where the targeted object appears like a dot and the stars in the background like trails. The sampling is limited by the framerate of the camera or the minimal time to see the difference between the dot and the train which depends on the tracking motion.

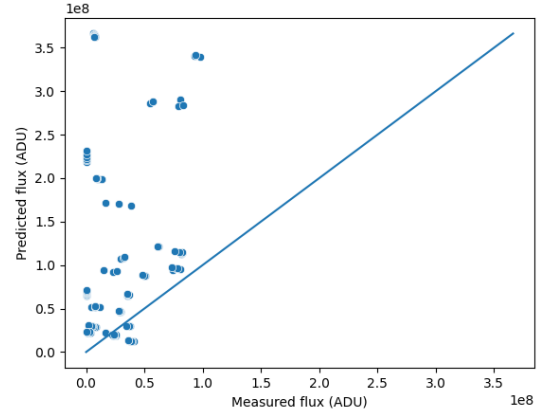


Figure 5. Difference between predicted and measured streak flux for observations of JASON 3 (#41240) carried out throughout 2022.

In Figure 9, the concatenated flux variation measured along streak a consecutive serie of image during the passage of the satellite in the field of view is plotted. The observed satellite is Ajisai (#16908), a sphere dedicated to laser ranging measurements.

## 4. PERFORMANCES OF LARGER TELESCOPES

Once the model fitted based on the observations, mostly regarding the albedo value of each satellite, it is possible to extrapolate it to larger telescopes in order to assess their performances, keeping in mind that the objective at hand is to determine the minimum space object size observable by a larger telescope. The aim is to extract the dimensions of the telescope, i.e focal length, aperture, central obstruction ratio, to manufacture it.

The focal ratio is the most important parameter, as it influences directly the field of view available. Increasing it allows to passively survey a larger region of the sky at once. One of the most challenging issues is the deformation at the edge of the FOV, as reducing the focal ratio increases the deformation. Nevertheless, it is still possible to overcome this issue, by revisiting optical concepts such as the Mangin mirror, or by combining basic concepts like Willstrop-Mersenne-Schmidt.

Regarding the observable size limit of space objects, the aperture diameter combined with the central obstruction ratio are the most critical criteria. Increasing the the aperture diameter and reducing the central obstruction ratio allows to collect more light, raising the sensitivity.

In the end, using a larger telescope comes down to increasing the SNR of satellites, as the signal produced by the space object and the background is dependent on the aperture surface and the focal ratio. Thus, by synthetically reducing the size of JASON 3 to converge to the

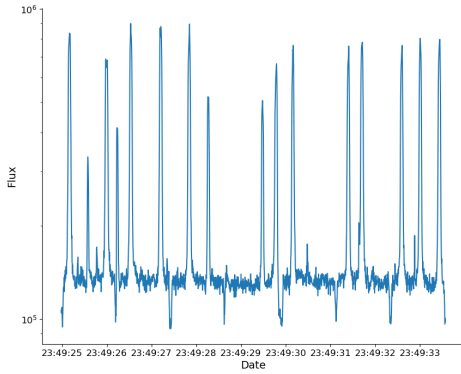


Figure 6. Concatenated brightness variation with flux measured along a streak of a serie of consecutive images obtained during the passage of the space object in the field of view.

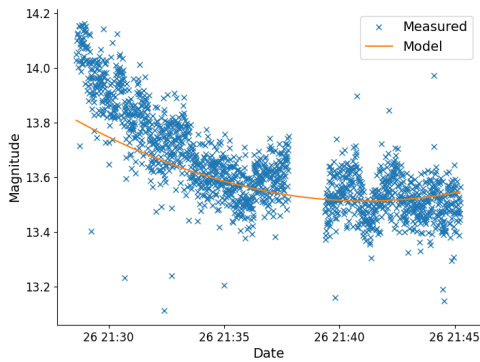


Figure 7. Light curve of the satellite Lageos (#8820) obtained with a tracking over 15 minutes.

limiting SNR allowing streak detection, we can estimate the size limit of any telescope. This is shown in Figure 8: the original dimensions of JASON 3 are  $3.7 \times 1.9 \times 9.7$  m, but to produce the same SNR with the WMS1000, a theoretical telescope with an aperture of 1000 mm, a focal ratio of 0.8 and a central obstruction of 66%, the size of JASON 3 needs to be reduced by more than 50%. This yields a new synthetic size of  $1.85 \times 0.95 \times 4.85$  m.

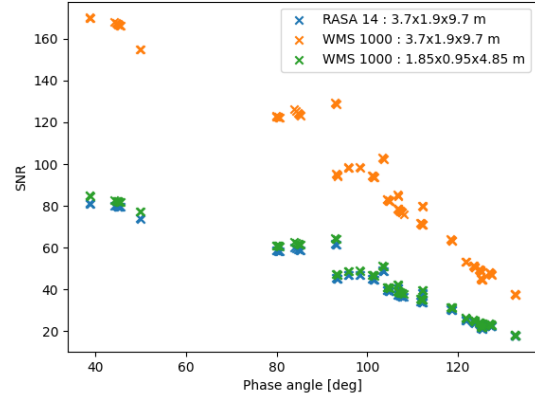


Figure 8. SNR according to phase angle. For a given SNR from RASA 14 observations, the WMS 1000 is twice as efficient regarding size limit.

## 5. ATTITUDE MODEL

The photometric model described can be improved by taking into account the attitude of the satellite. The Lambert sphere model can be replaced by the Bi-Reflective Diffuse Function (BRDF), accounting for the orientation of each surface of the satellite and its shape [6]. In Figure 9, the light curve of the upper-stage ATLAS 5 CENTAUR R/B is provided and the rotation period is extracted with the Lomb-Scargle method [4]. The next step will be to include the BRDF computation in the photometric model.

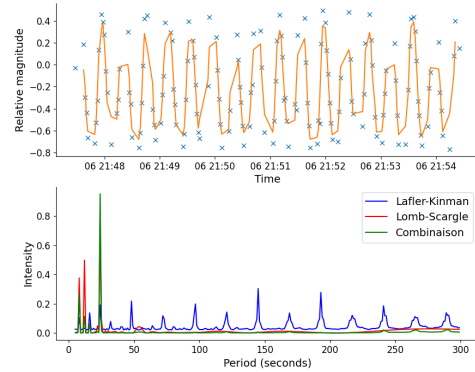


Figure 9. Light curve of the upper-stage ATLAS 5 CENTAUR R/B (#40295) obtained with tracking.

## 6. CONCLUSION

In this paper we have extended our previous works about the modeling of the photon chain in the case of optical sensors. In Petit et al. (2021) [2], the description of

the complete model has been introduced but some discrepancies appear when we compare photometric measurements and the values given by the model. Means of improvement have been investigated like the sky background modeling, the camera characterisation, and the dependency to the space object orientation was discussed.

A good agreement between the model and the measures was found for the sky background flux measured and the streak flux of space objects. However some outliers still appear. The theoretical flux, especially, is overestimated. The model is also compared with photometric measurements during a continuous space object tracking, i.e. with a light curve. An agreement was found with slight discrepancy at the beginning of the light curve probably due to the sensibility to the phase angle as suggested by authors in the past.

In the future, accumulation of data will help us to improve the model introduced in this paper confirming hypothesis and corrections. Major points are identified: the limits of the Lambert sphere model and the use of the BRDF, the role of the Earthshine as suggested by Cognion (2013) [7], or the non-linearity of the camera.

## REFERENCES

1. Ackermann, Mark R., et al., (2015) A systematic examination of ground-based and space-based approaches to optical detection and tracking of artificial satellites.
2. Petit, A., Lucken, R., Tarrieu, H., Giolito, D., Cavadore, C., Lépine, T. (2021). Share My Space Multi-telescope Observation Stations Performance Assessment.
3. Krisciunas, K., Schaefer, B. E. (1991). A model of the brightness of moonlight. *Publications of the Astronomical Society of the Pacific*, 103(667), 1033.
4. Šilha, J., Pittet, J. N., Hamara, M., Schildknecht, T. (2018). Apparent rotation properties of space debris extracted from photometric measurements. *Advances in space research*, 61(3), 844-861.
5. Hejduk, M. D. (2011, September). Specular and diffuse components in spherical satellite photometric modeling. In *Proceedings of the Advanced Maui Optical and Space Surveillance Technologies Conference* (pp. 1-11).
6. Bradley, B. K., Axelrad, P. (2014, May). Lightcurve inversion for shape estimation of geo objects from space-based sensors. In *Univ. of Colorado. International Space Symposium for Flight Dynamics*.
7. Cognion, R. (2013). Observations and modeling of GEO satellites at large phase angles. *AMOS Proceedings*.